



RESEARCH ARTICLE

An Isotope (^{18}O , ^{15}N , and ^2H) Technique to Investigate the Metal Ion Interactions Between the Phosphoryl Group and Amino Acid Side Chains by Electrospray Ionization Mass Spectrometry

Xiang Gao,¹ Xiaomei Hu,¹ Jun Zhu,² Zhiping Zeng,¹ Daxiong Han,³ Guo Tang,¹ Xiantong Huang,¹ Pengxiang Xu,¹ Yufen Zhao^{1,3}

¹Department of Chemistry and The Key Laboratory for Chemical Biology of Fujian Province, College of Chemistry and Chemical Engineering, Xiamen University, Xiamen, 361005, People's Republic of China

²Department of Chemistry and Fujian Provincial Key Laboratory of Theoretical and Computational Chemistry, College of Chemistry and Chemical Engineering, Xiamen University, Xiamen, 361005, People's Republic of China

³Department of Medicine, Medical College, Xiamen University, Xiamen, 361005, People's Republic of China

Abstract

Cationic metal ion-coordinated *N*-diisopropoxyphosphoryl dipeptides (DIPP-dipeptides) were analyzed by electrospray ionization multistage tandem mass spectrometry (ESI-MSⁿ). Two novel rearrangement reactions with hydroxyl oxygen or carbonyl oxygen migrations were observed in ESI-MS/MS of the metallic adducts of DIPP-dipeptides, but not for the corresponding protonated DIPP-dipeptides. The possible oxygen migration mechanisms were elucidated through a combination of MS/MS experiments, isotope (^{18}O , ^{15}N , and ^2H) labeling, accurate mass measurements, and density functional theory (DFT) calculations at the B3LYP/6-31 G(d) level. It was found that lithium and sodium cations catalyze the carbonyl oxygen migration more efficiently than does potassium and participation through a cyclic phosphoryl intermediate. In addition, dipeptides having a C-terminal hydroxyl or aromatic amino acid residue show a more favorable rearrangement through carbonyl oxygen migration, which may be due to metal cation stabilization by the donation of lone pair of the hydroxyl oxygen or aromatic π -electrons of the C-terminal amino acid residue, respectively. It was further shown that the metal ions, namely lithium, sodium, and potassium cations, could play a novel directing role for the migration of hydroxyl or carbonyl oxygen in the gas phase. This discovery suggests that interactions between phosphorylated biomolecules and proteins might involve the assistance of metal ions to coordinate the phosphoryl oxygen and protein side chains to achieve molecular recognition.

Key words: Oxygen migration, Isotope labeling ESI-MS/MS, N-Phosphoryl dipeptide, Metal ion

Electronic supplementary material The online version of this article (doi:10.1007/s13361-010-0069-5) contains supplementary material, which is available to authorized users.

Correspondence to: Pengxiang Xu; e-mail: xpengxiang@xmu.edu.cn

Introduction

It has been shown that *N*-phosphoryl amino acids (NPAAAs) and peptides are chemically active species [1–3], which might be not only related to the prebiotic synthesis of proteins and nucleic acids [4–6] but also the

Received: 9 January 2010

Revised: 24 December 2010

Accepted: 28 December 2010

Published online: 1 February 2011

“Mini-Kinase” model to elucidate the phosphoryl transfer mechanism for the phosphorylation/dephosphorylation of proteins [7, 8]. In addition, NPAAAs might also be considered as novel chemical models for the investigation of interactions between phosphoryl groups (P=O) and biomolecules. For example, in solution phase, *N*-phosphoryl α -amino acids could be transformed into both peptides and nucleic acids via a five-membered cyclic pentacoordinate phosphoric-amino acid mixed anhydride, while the homo-isomers *N*-phosphoryl β - or γ -amino acids are inert [4, 9]. The β -carboxylic group of *N*-phosphoryl aspartic acid but not the γ -carboxylic of *N*-phosphoryl glutamic acid show neighboring group effects [10, 11]. Similarly, the catalytic activity of the side-chain β -OH from serine is higher than the γ -OH of the homoserine [12, 13]. In addition, several natural and synthetic *N*-phosphoryl peptides, such as *N*-phosphoryl-leucyl-tryptophan and *N*-phosphoryl-leucyl-phenylalanine, are potent reversible inhibitors of metalloproteinases [14]. All these examples illustrate that phosphoryl groups play significant roles in peptide chemistry. It goes without saying that phosphoryl groups are common constituents in living cells and control many biochemical events [15], such as enzyme regulation, phospho-signaling, and protein/protein association [16–18]. Hence, studying the properties of phosphoryl amino acids and peptides as the smallest chemical models in the liquid phase or the gas phase can provide some significant clues for understanding the behavior of phosphorylated biomolecules.

Electrospray ionization tandem mass spectrometry (ESI-MSⁿ) offers a suitable tool for the study of novel reactions performed in the gas phase. Since its introduction by Yamashita and Fenn in 1984 [19], ESI-MS has been extensively used in biological science, e.g., molecular recognition and supramolecular chemistry [20], noncovalent macromolecule–ligand interactions [21], protein phosphorylation [22], and sequencing of peptides or proteins [23, 24]. Furthermore, metal ions are known to play an essential role in biological systems by interaction with proteins or phosphorylated proteins. For instance, there have been a great many studies on the gas phase chemistry of complexes of the alkali metal ions with amino acids or simple peptides by ESI-MS in the past decade, such as the dissociation pathways of cationic peptides [25, 26] and metal ion binding affinities with a number of amino acids and simple peptides [27]. However, to the best of our knowledge, there are no viable model systems for the investigations of the interaction between the metal ions and phosphorylated biomolecules in the gas phase.

In our previous work, multistage ESI-MS combined with *N*-phosphoryl derivatization has been used for peptide sequencing [28, 29]. Several unusual rearrangement reactions for *N*-phosphoryl amino acids and peptide derivatives have been observed, such as rearrangement of P–N to P–O bonds [30], carbonyl oxygen migration [31], and methoxy group migration [32]. From structural analysis of the *N*-phosphoryl amino acids and peptides, it is apparent that this

series of compounds possess a unique advantage of combining together the metal ion, phosphoryl group (P=O bond) and amino acid. Therefore, complexes of *N*-phosphoryl amino acids or peptides with metal ions could be considered as model systems for studies of the metal ion interactions between the phosphoryl group and various types of amino acid residue. In this paper, stable-isotope labeling strategies (¹⁸O, ¹⁵N, and ²H labeling) were applied to investigate the novel rearrangement reaction of the alkali metal ion adducts of *N*-phosphoryl dipeptides by ESI-MSⁿ. It was found that metal cations of lithium, sodium, and potassium could catalyze the hydroxyl oxygen or carbonyl oxygen migration under collision-induced dissociation (CID) conditions.

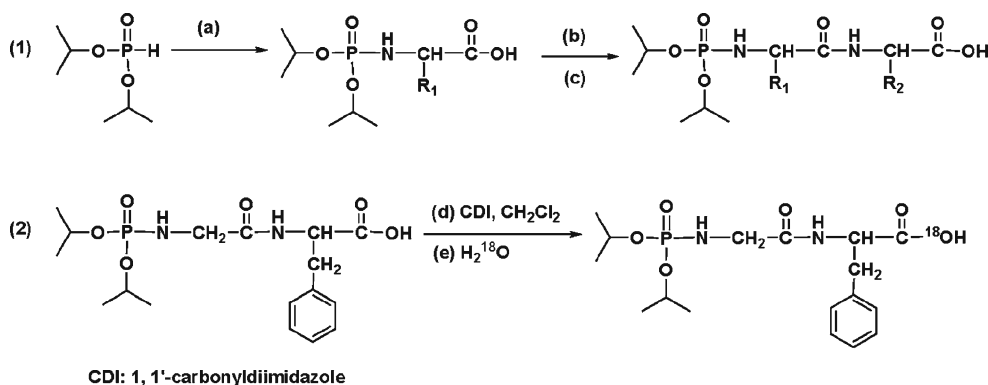
Experimental

Materials and Sample Preparation

H-¹⁵N-Gly-OH (98 at% ¹⁵N), H₂¹⁸O (98 at% ¹⁸O), D₂O (99.9 at% D), and CH₃OD (99.9 at% D) were obtained from Cambridge Isotope Laboratories (Andover, MA, USA). L-amino acids were purchased from GL Biochem. Ltd. (Shanghai, China). Compounds 1–17 were synthesized by literature methods with yields of 60%–70% (Scheme 1) [33, 34]. DIPP-¹⁵N-Gly-Phe was synthesized using H-¹⁵N-Gly-OH as start material. DIPP-Gly-Phe-¹⁸OH was prepared by a one-pot procedure (Scheme 1) [35]: *N*-diisopropylphosphoryl Gly-Phe-OH (0.5 mmol) was dissolved in anhydrous CH₂Cl₂ (5 mL) under argon atmosphere. To this solution was slowly added 1, 1'-carbonyldiimidazole (CDI, 0.6 mmol) at room temperature and stirred for about 1 h until no further CO₂ gas evolution was observed. Then, H₂¹⁸O (2 mmol, 40 μ L) was added to the reaction mixture and stirred for another 2 h. The solvents were removed under reduced pressure, and the residue was purified by silica gel chromatography using EtOAc-MeOH (20:1) as eluent. The DIPP-Gly-Phe-¹⁸OH was obtained as a colorless oil in high yield. All compounds synthesized were identified by ³¹P NMR, ¹H NMR, ¹³C NMR, and ESI-MS. NMR data for DIPP-Gly-Phe (Entry 1): ³¹P NMR (162 MHz, CDCl₃): δ =6.06 ppm. ¹H NMR (400 MHz, CDCl₃): δ =1.26–1.32 (m, 12 H), 2.99 (dd, *J*=6.4, 14.0 Hz, 1 H), 3.19 (dd, *J*=5.6, 14.0 Hz, 1 H), 3.52–3.58 (m, 2 H), 4.23 (dd, *J*=8.4, 16.4 Hz, 1 H), 4.50–4.60 (m, 2 H), 4.92 (dd, *J*=6.0, 14.0 Hz, 1 H), 7.11–7.28 ppm (m, 5 H). ¹³C NMR (100 MHz, CDCl₃): δ =173.7, 169.6 (d, *J*=7.4 Hz), 136.5, 129.4, 128.3, 126.8, 72.1 (d, *J*=5.8 Hz), 72.0 (d, *J*=5.7 Hz), 52.9, 44.6, 37.8, 23.72, 23.67, 23.60, 23.5 ppm.

Mass Spectrometry Conditions

Mass spectra were acquired in the positive ion mode using a Bruker Esquire 3000Plus ion trap mass spectrometer (Bruker Daltonics Inc., Billerica, MA, USA) equipped with a gas nebulizer probe capable of analysis to *m/z* 6000. Nitrogen



Scheme 1. General strategy for the synthesis of *N*-diisopropoxyphosphoryl dipeptides. Reaction conditions: **(a)** Amino acid (or ^{15}N labeled amino acid), CCl_4 , H_2O , triethylamine, EtOH, ice-salt bath, 6 h; **(b)** Amino acid methyl esters, Ph_3P , C_2Cl_6 , triethylamine, CH_2Cl_2 , ice-salt bath, 2 h; **(c)** $0.5 \text{ mol} \cdot \text{L}^{-1}$ NaOH, room temperature, 1 h

gas was used at a flow-rate of $4 \text{ L} \cdot \text{min}^{-1}$. The nebulizer pressure was 8 psi and the electrospray capillary was typically held at 4 kV. The heated capillary temperature was $250 \text{ }^\circ\text{C}$. Samples in methanol at $\sim 0.01 \text{ mg} \cdot \text{mL}^{-1}$ were ionized by ESI and infused continuously into the ESI chamber at a flow-rate of $4 \text{ } \mu\text{L} \cdot \text{min}^{-1}$ by a Cole-Parmer 74900 syringe pump (Cole-Parmer Instrument Co. Vernon Hills, IL, USA). The scan range was generally from m/z 50 to 800. Five scans were averaged for each spectrum. The precursor ions $[\text{M}+\text{H}]^+$, $[\text{M}+\text{Li}]^+$, $[\text{M}+\text{Na}]^+$, and $[\text{M}+\text{K}]^+$ were selected using an isolation width of 1.0 to 1.5 mass to charge (m/z) units and analyzed by multistage tandem mass spectrometry (MS^n) through collisions with helium. The fragmentation amplitude values were 0.3 to 0.8 V and the fragmentation time was 40 ms.

High-resolution tandem mass spectrum of deuterium labeled DIPP-Gly-Phe was recorded on a Bruker APEX-Ultra Fourier transform ion cyclotron resonance mass spectrometer equipped with an analytic electrospray source in the positive ion mode. Deuterium-labeled experiment: DIPP-Gly-Phe (1 mg) was incubated with $\text{D}_2\text{O}/\text{CH}_3\text{OD}$ (2 mL, 1:1, vol/vol) overnight at room temperature for exchange of labile protons. An aliquot of the reaction mixture (10 μL) was diluted with CH_3OD (1 mL) and analyzed by ESI-HRMS/MS. Acquisition parameter: Drying gas temperature: $180 \text{ }^\circ\text{C}$; drying gas flow rate: $5.0 \text{ L} \cdot \text{min}^{-1}$; nebulizer gas flow rate: $1.0 \text{ L} \cdot \text{min}^{-1}$; ion accumulation time: 2.0 s. The following voltages were used: capillary entrance voltage (4.3 kV), end plate (3.8 kV), skimmer 1 (36 V), and collision energy (13.5 V). The scan range was from m/z 100 to 700. The sample dissolved in CH_3OD was introduced into the source at a flow rate of $4 \text{ } \mu\text{L} \cdot \text{min}^{-1}$. The three deuterium atoms labeled $[\text{d}_3\text{-DIPP-Gly-Phe}+\text{Na}]^+$ ion at m/z 412.1718 was isolated with a width of 0.1 mass to charge unit. Twenty scans were averaged for each spectrum. Other high-resolution mass spectra were recorded on a Shimadzu liquid chromatograph/mass spectrometry-ion trap-time-of-flight (LC-IT-TOF) (Shimadzu, Kyoto, Japan) equipped with an analytic electrospray source in the positive ion mode. Probe voltage was 4.5 kV and scan range was from m/z 50 to 800.

The sample in CH_3OH was introduced into the source at a flow rate of $10 \text{ } \mu\text{L} \cdot \text{min}^{-1}$. The nebulizing gas flow was $0.5 \text{ L} \cdot \text{min}^{-1}$ and the ion accumulation time was 10.0 ms.

Calculations

Molecular geometries of all species in this work were optimized at the B3LYP/6-31 G(d) level [36–38]. Frequency calculations at the same level of theory have also been performed to confirm that all stationary points were minima (no imaginary frequency) or transition states (one imaginary frequency). Calculations of intrinsic reaction coordinates (IRC) [39, 40] were also performed on transition states to confirm that such structures are indeed connecting two minima. To examine the effect of basis sets, we also employed a larger basis set, 6-311 G(d, p), to perform single-point energy calculations for several selected structures. The additional calculations show that the basis set dependence is small. For example, using the smaller basis set, the relative energies of lithiated IIa, TS-ab, and IIb (Figure 4) are 0.0, 42.6, and $9.9 \text{ kcal} \cdot \text{mol}^{-1}$, respectively. Using the larger basis set, the relative energies of these species are 0.0, 42.1, and $8.5 \text{ kcal} \cdot \text{mol}^{-1}$, respectively. Similarly, using the smaller basis set, the relative energies of sodiated IIa, TS-ab, and IIb (Figure 4) are 0.0, 48.7 and $16.5 \text{ kcal} \cdot \text{mol}^{-1}$, respectively. Using the larger basis set, the relative energies of these sodiated species are 0.0, 47.0, and $14.1 \text{ kcal} \cdot \text{mol}^{-1}$, respectively. All calculations were performed with the Gaussian 03 software package [41].

Results and Discussion

The characteristic fragmentations in ESI-MS of *N*-phosphoryl peptides 1–17 are compiled in Table 1. This illustrates that these group of compounds follow a common dissociation pathway. As a representative, the ESI- MS^n positive ion mass spectral fragmentation pattern of *N*-diisopropoxyphosphoryl Gly-Phe dipeptide (DIPP-Gly-Phe, Entry 1) is analyzed in detail. The multiple-stage CID

Table 1. Partial ESI-MS/MS data for *N*-diisopropoxyphosphoryl dipeptides. The relative abundance percentages are noted in parentheses. (Cat⁺ = H⁺, Li⁺, Na⁺, and K⁺)

Entry and compound	Precursor ion, <i>m/z</i>	Species [M+Cat] ⁺	[M+Cat -42] ⁺	[M+Cat -102] ⁺	[M+Cat -164] ⁺	Rearrangement ions	
						I	II
1 DIPP-Gly-Phe	393	[M+Li] ⁺	351(100)	291(3)	229(4)	246(15)	211(92)
	409	[M+Na] ⁺	367(100)	307(11)	245(11)	262(24)	227(99)
	425	[M+K] ⁺	383(100)	323(8)	261(0)	278(6)	243(6)
2 DIPP- ¹⁵ N-Gly-Phe	387	[M+H] ⁺	345(100)	285(16)	223(0)	240(0)	205(0)
	394	[M+Li] ⁺	352(100)	292(4)	230(3)	247(16)	212(90)
	410	[M+Na] ⁺	368(96)	308(12)	246(11)	263(25)	228(100)
	426	[M+K] ⁺	384(100)	324(9)	262(0)	279(7)	244(7)
3 <i>d</i> ₃ -DIPP-Gly-Phe	388	[M+H] ⁺	346(100)	286(14)	224(0)	241(0)	206(0)
	412.1718	[M+Na] ⁺	370.1243	309.0600	248.1096	264.0954	228.0862
4DIPP-Gly-Phe- ¹⁸ OH	411	[M+Na] ⁺	-	310.0662	-	-	229.0925
			369(100)	309(13)	247(10)	264(13)	229(51)
5 DIPP-Ala-Ala	331	[M+Li] ⁺	289(100)	229(0)	167(5)	260(11)	149(21)
	347	[M+Na] ⁺	305(100)	245(6)	183(8)	276(24)	165(7)
	363	[M+K] ⁺	321(100)	261(0)	199(0)	292(0)	181(0)
	325	[M+H] ⁺	283(100)	223(24)	161(0)	254(0)	143(0)
6 DIPP-Ala-Val	359	[M+Li] ⁺	317(100)	257(0)	195(5)	260(48)	177(22)
	375	[M+Na] ⁺	333(49)	273(5)	211(5)	276(40)	193(5)
	391	[M+K] ⁺	349(100)	289(21)	227(45)	292(4)	209(0)
	353	[M+H] ⁺	311(97)	251(27)	189(0)	254(0)	171(0)
7 DIPP-Ala-Leu	373	[M+Li] ⁺	331(100)	271(0)	209(0)	260(26)	191(20)
	389	[M+Na] ⁺	347(60)	287(7)	225(8)	276(32)	207(6)
	405	[M+K] ⁺	363(100)	303(5)	241(0)	292(12)	223(0)
	367	[M+H] ⁺	325(93)	265(15)	203(0)	254(0)	185(0)
8 DIPP-Ala-Phe	407	[M+Li] ⁺	365(100)	305(5)	243(3)	260(16)	225(97)
	423	[M+Na] ⁺	381(96)	321(11)	259(10)	276(28)	241(100)
	439	[M+K] ⁺	397(100)	337(9)	275(4)	292(7)	257(9)
	401	[M+H] ⁺	359(100)	299(17)	237(0)	254(0)	219(0)
9 DIPP-Phe-Ala	407	[M+Li] ⁺	365(100)	305(0)	243(7)	336(15)	225(76)
	423	[M+Na] ⁺	381(68)	321(50)	259(10)	352(23)	241(55)
	439	[M+K] ⁺	397(29)	337(2)	275(3)	368(3)	257(2)
	401	[M+H] ⁺	359(100)	299(18)	164(0)	254(0)	219(0)
10 DIPP-Phe-Gly	409	[M+Na] ⁺	367(78)	307(13)	245(24)	352(1)	227(66)
11 DIPP-Phe-Val	451	[M+Na] ⁺	409(39)	349(5)	287(14)	352(100)	269(57)
12 DIPP-Val-Phe	451	[M+Na] ⁺	409(100)	349(12)	287(12)	304(23)	269(92)
13 DIPP-Leu-Phe	465	[M+Na] ⁺	423(100)	363(12)	301(11)	318(19)	283(83)
14 DIPP-Ala-Ser	363	[M+Na] ⁺	321(100)	261(7)	199(8)	276(8)	181(76)
15 DIPP-Ala-Thr	377	[M+Na] ⁺	335(89)	275(7)	213(10)	276(16)	195(100)
16 DIPP-Leu-Ser	405	[M+Na] ⁺	363(100)	303(10)	241(5)	318(10)	223(82)
17 DIPP-Val-Ser	391	[M+Na] ⁺	349(100)	289(10)	227(7)	304(10)	209(95)

spectra of native and isotope labeled DIPP-Gly-Phe are shown in Figure 1 and Figure 2.

The fragmentation patterns of the sodium ion DIPP-Gly-Phe (1) [M+Na]⁺ (Figure 1a) at *m/z* 409 were determined as shown in Scheme 2. It can be seen that the precursor ion [M+Na]⁺ at *m/z* 409 can lose propylene to form an abundant daughter ion at *m/z* 367, which in turn fragments to produce an ion at *m/z* 307 by successive loss of propylene (42 Da) and water (18 Da) through Path A (Figure 1b). The fragmentation reaction is typical of positive-ion ESI-MS/MS of DIPP-amino acids and peptides. Furthermore, by Path B, the fragment ion at *m/z* 262 (Ion I), corresponding to [DIPP-Gly+Na]⁺, could be generated through losing a C-terminal phenylalanine residue by transfer of carboxyl oxygen from the original C-terminus of DIPP-Gly-Phe to the new C-terminal carboxylic acid group of DIPP-Gly. In order to identify this product ion at *m/z* 262, its MS³ showed that fragment ions at *m/z* 220 and 178 were formed

by the loss of one or two molecules of propylene, respectively (Figure 1d). Moreover, a characteristic rearrangement ion for sodium cationized DIPP-Gly is observed at *m/z* 163, which may be produced from a cyclic pentacoordinated phosphoric-carboxylic intermediate leading to P–N to P–O migration [30]. High-resolution ESI-MS/MS (Table 2) indicates that the exact mass of ion I was 262.0824, corresponding to elemental composition C₈H₁₈NNaO₅P, which could be formed from the parent ion [M+Na]⁺ at *m/z* 409.1486 by the loss of a neutral C-terminal phenylalanine residue with molecular weight of 147.0662 (Theoretical mass: 147.0684). However, the formation of other novel fragment ion at *m/z* 227, formed from the parent ion at *m/z* 307 by the loss of a neutral molecule 80 Da (HPO₃) as shown in Figure 1c, cannot easily be explained. High-resolution mass analysis of this ion at *m/z* 227.0978 Da indicates an atomic composition of C₁₁H₁₂N₂NaO₂, which corresponds within 1 ppm to the proposed structure ion II as shown in Scheme 7.

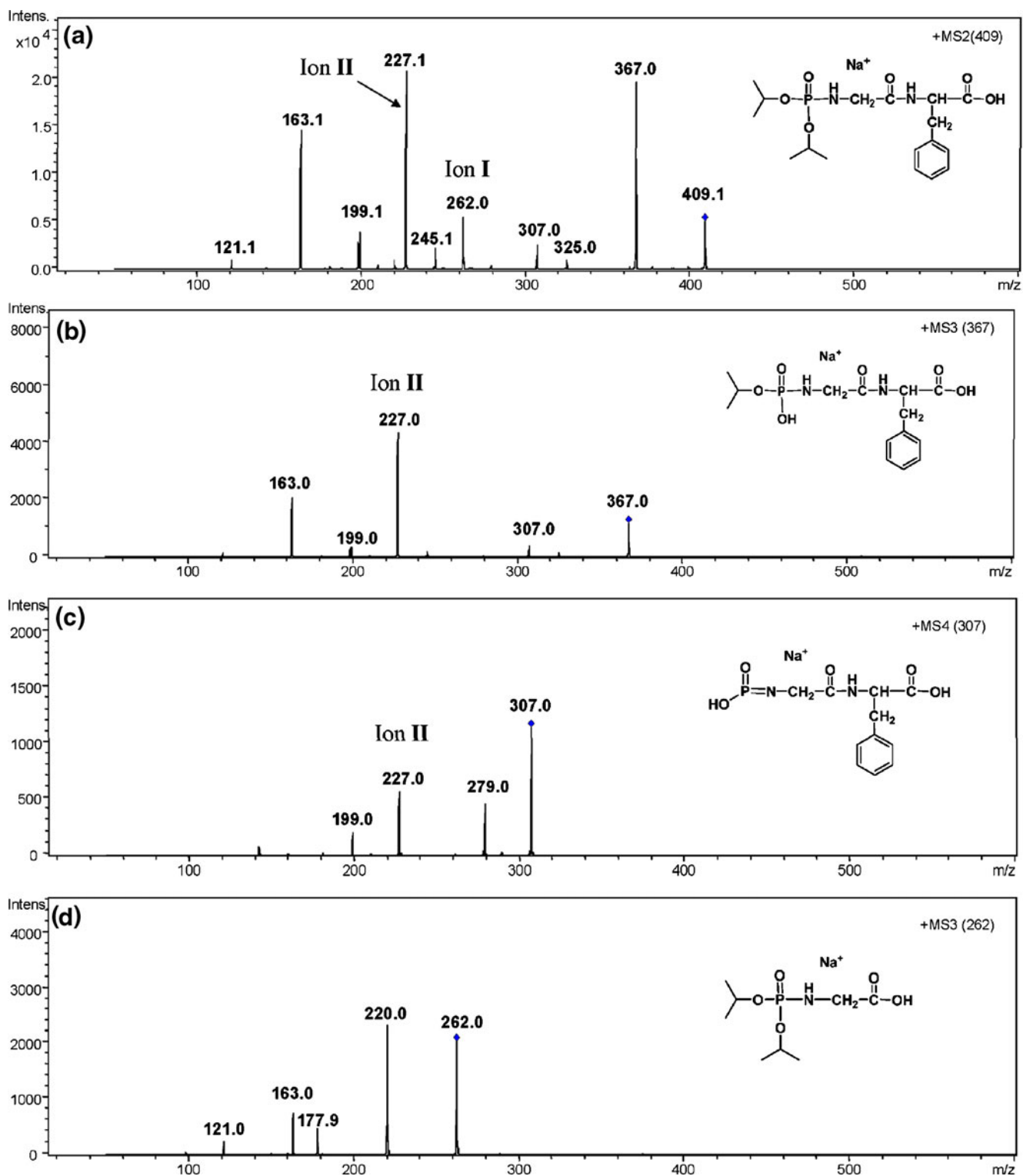


Figure 1. Positive ion ESI tandem mass spectra of DIPP-Gly-Phe (Entry 1). **(a)** ESI-MS/MS of the sodium adducts of DIPP-Gly-Phe at m/z 409; **(b)** ESI-MS³ of the $[M+Na - 42]^+$ ion at m/z 367; **(c)** ESI-MS⁴ of the $[M+Na - 102]^+$ ion at m/z 307; **(d)** ESI-MS³ of the rearrangement ion at m/z 262

In order to clarify the structures of these two novel product ions at m/z 227 (ion II) and 262 (ion I), isotopic labeling experiments were conducted. First, ^{15}N -labeled DIPP-Gly-Phe dipeptide (DIPP- ^{15}N -Gly-Phe) was synthe-

sized and analyzed by ESI-MS/MS as shown in Figure 2a. The signals corresponding to the rearrangement ions I and II, observed at m/z 262 and 227 with the unlabeled material, are shifted by 1 u to m/z 263 and 228, respectively, which

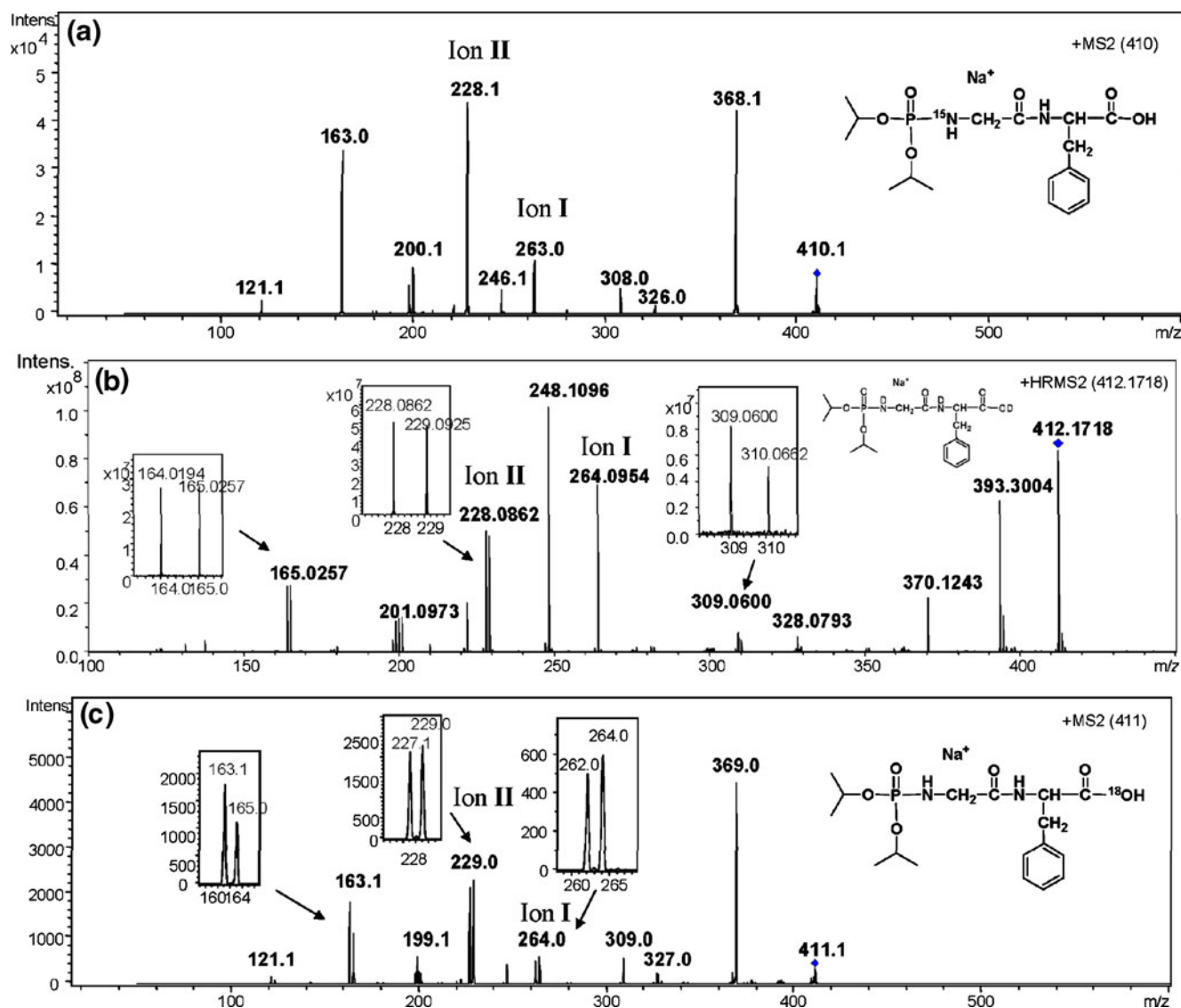


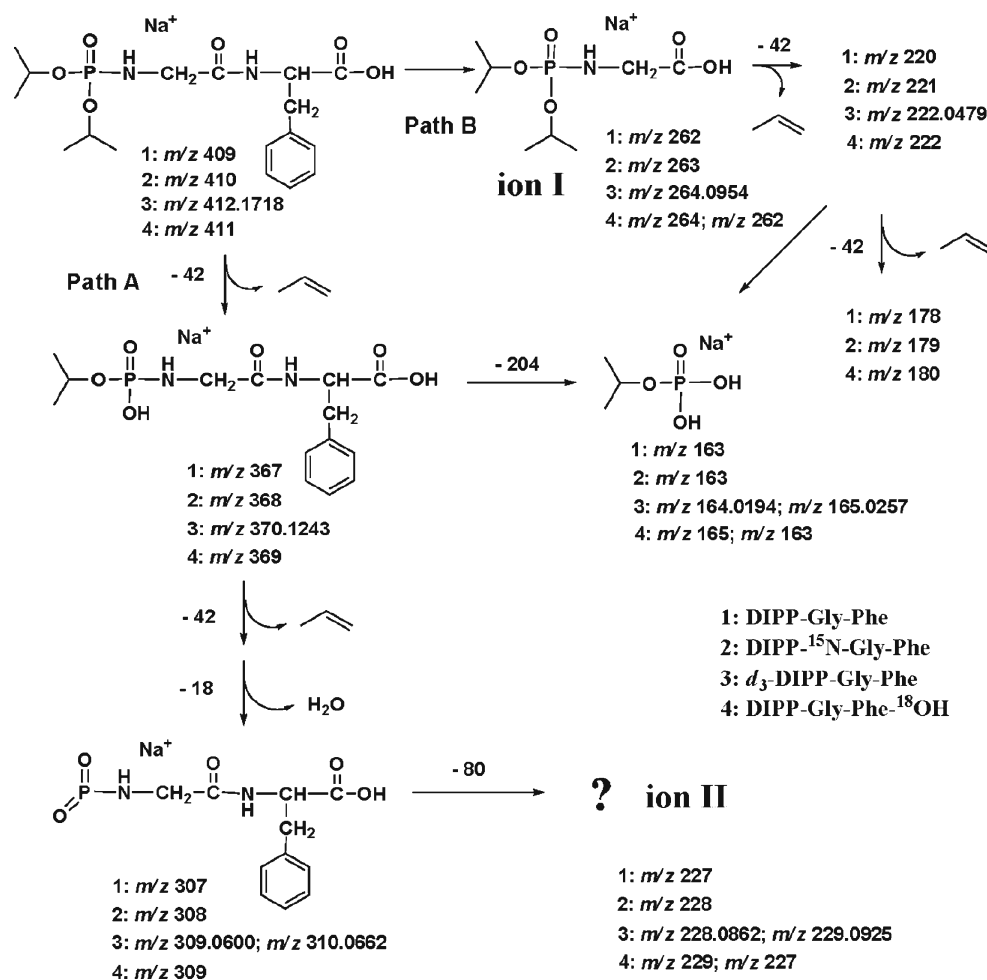
Figure 2. Positive ion ESI-MS/MS spectra of the $[M+Na]^+$ of the isotope labeled DIPP-Gly-Phe (^{18}O , ^{15}N , and 2H). **(a)** ESI-MS/MS of isotope labeled DIPP- ^{15}N -Gly-Phe ion at m/z 410 (Entry 2); **(b)** High resolution ESI-MS/MS of deuterium-labeled DIPP-Gly-Phe ion at m/z 412.1718 (d_3 -labeled, Entry 3); **(c)** ESI-MS/MS of isotope labeled DIPP-Gly-Phe- ^{18}OH ion at m/z 411 (Entry 4)

suggested that both fragment ions contained the nitrogen atom of the glycine residue derived from parent compound DIPP-Gly-Phe. Furthermore, according to the general “N rule” in the elemental analysis, the product ion I should have one nitrogen atom because of the molecular weight of the fragment at m/z 262 is odd (239 Da) after subtracting 23 Da of Na. On the contrary, the Na^+ adduct ion II at m/z 227 with even molecular weight (204 Da) should have two nitrogen atoms.

Secondly, all amino, amide, and acid groups of the sodiated DIPP-Gly-Phe were labeled with deuterium atoms via solution-phase hydrogen/deuterium exchange before the sample was injected into the ESI-FT-ICR-MS. The d_3 -labeled $[M+Na]^+$ ion at m/z 412.1718 was subjected to high resolution ESI-MS/MS. As shown in Figure 2b, compared with ion I of the native DIPP-Gly-Phe at m/z 262, ion I of d_3 -labeled DIPP-Gly-Phe appears as a mass

peak at m/z 264.0954 with a 2 u shift, which implies that the ion I has two active hydrogen atoms. Meanwhile, the rearrangement ion II could also contain two exchangeable protons since two mass peaks at m/z 228.0862 (d_1 -) and m/z 229.0925 (d_2 -) are observed. As shown in Scheme 3, the d_3 -labeled $[M+Na - 84]^+$ ion at m/z 328.0793 could lose a molecule of HDO and H_2O to form two daughter ions at m/z 309.0600 and m/z 310.0662 respectively, which subsequently fragmented to produce ions at m/z 228.0862 and 229.0925 by elimination of a molecule of deuterium-labeled metaphosphate (DPO_3).

Thirdly, the C-terminal [$^{18}O_1$]-labeled DIPP-Gly-Phe- ^{18}OH 4 was synthesized and analyzed by ESI-MS/MS (Figure 2c and Figure 3). As shown in Figure 2c, a mass increment of 2 Da of the precursor ion from m/z 409 to m/z 411 implies the exchange of one ^{16}O with one ^{18}O .



Scheme 2. Fragmentation pathways of the sodium adducts of DIPP-Gly-Phe (Entry 1), DIPP-¹⁵N-Gly-Phe (Entry 2), deuterium labeled *d*₃-DIPP-Gly-Phe (Entry 3), and DIPP-Gly-Phe-¹⁸OH (Entry 4)

However, it is possible that the H₂¹⁸O can attack the C=O of Glycine residue or P=O group and causes ¹⁸O labeling at these sites when carried out the labeled experiments. In order to specify the location of exchange, the protonated DIPP-Gly-Phe-¹⁸OH at m/z 389 that was shifted 2 Da from the native protonated DIPP-Gly-Phe at m/z 387 was studied by ESI-MS/MS (Figure 3). Furthermore, the fragmentation pathways of the protonated DIPP-Gly-Phe-¹⁸OH were compiled in Scheme 4. Considering the Scheme 4, it was found that the precursor ion at m/z 389 could lose the neutral H₂¹⁸O+CO or H₂O+C¹⁸O to produce the single mass peak at m/z 341, indicating that the ¹⁸O labeling occurred only at the C-terminal carboxylic acid group. Indeed, because of the equivalence of the two C-terminal oxygens, it was reasonable to find that ion I appeared at m/z 262 and 264 in a ratio of 1:1, corresponding to unlabeled and [¹⁸O₁]-labeled [DIPP-Gly+Na]⁺ ions, respectively. It indicates that one of the C-terminal carboxyl oxygens migrates to the new C-terminus (Scheme 5a). However, it is quite surprising to find that ion II also appears as two peaks at m/z 227 (unlabeled) and 229 ([¹⁸O₁]-labeled) in a ratio of approximately 1:1 (Figure 2c), which might arise from intramolecular ¹⁸O exchange without peptide bond cleavage in the gas phase as

shown in Scheme 5b [42]. Thus, the data from the isotope-labeled substrates, with respect to retention or elimination of the isotopes, gives structural information that can unambiguously identify the structures of the product ions.

Based on the experimental results, we propose two possible rearrangement mechanisms to account for the formation of ions I and II, respectively (Schemes 6 and 7). In one mechanism by chelation, the alkali metal ions could bring the amide carbonyl oxygen and carboxylic oxygen atom closer through an intermediate seven-membered ring Ia [43, 44]. Then the oxygen atom of the C-terminal carboxylic group could attack the carbonyl bond of the adjacent amide carbonyl nucleophilically to form an anhydride intermediate Ib with a five-membered ring. Subsequently, by C–N bond cleavage and by loss of CO and an imine, ion I, metallic ion adducts of DIPP amino acids, could be formed. Indeed, a similar reaction mechanism involved the concerted proton transfer and nucleophilic attack leading to a b-OH type ions has been investigated extensively [45–48]. The second mechanism for the generation of ion II is shown in Scheme 7, the metallic ion might be closely coordinated between the phosphoryl oxygen, carbonyl oxygen, and phenyl group

Table 2. High-resolution ESI-MS/MS data for the sodium adducts of DIPP-Gly-Phe (Entry 1), DIPP-Ala-Phe (Entry 8), and DIPP-Phe-Ala (Entry 9)

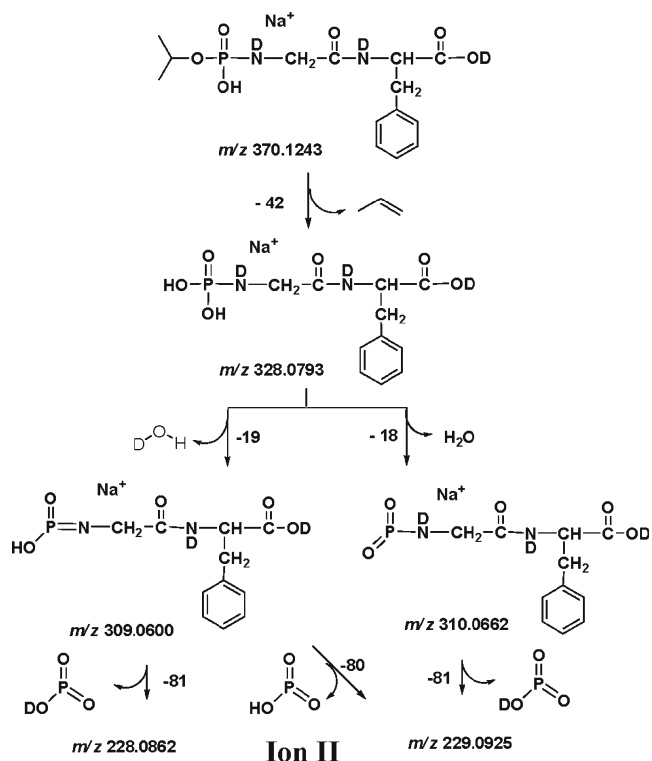
Compound		Precursor ion	Ion I	Ion II
DIPP-Gly-Phe (1)	<i>m/z</i>	409	262	227
	Theoretical mass (<i>m/z</i>)	409.1504	262.0820	227.0796
	Measured mass (<i>m/z</i>)	409.1486	262.0824	227.0798
	Relative error (ppm)	4.3	1.5	0.9
	Chemical formula	C ₁₇ H ₂₇ N ₂ NaO ₆ P ⁺	C ₈ H ₁₈ NNaO ₅ P ⁺	C ₁₁ H ₁₂ N ₂ NaO ₂ ⁺
DIPP-Ala-Phe (8)	<i>m/z</i>	423	276	241
	Theoretical mass (<i>m/z</i>)	423.1661	276.0977	241.0953
	Measured mass (<i>m/z</i>)	423.1661	276.0983	241.0951
	Relative error (ppm)	0.0	2.2	0.8
	Chemical formula	C ₁₈ H ₂₉ N ₂ NaO ₆ P ⁺	C ₉ H ₂₀ NNaO ₅ P ⁺	C ₁₂ H ₁₄ N ₂ NaO ₂ ⁺
DIPP-Phe-Ala (9)	<i>m/z</i>	423	352	241
	Theoretical mass (<i>m/z</i>)	423.1661	352.1290	241.0953
	Measured mass (<i>m/z</i>)	423.1661	352.1307	241.0938
	Relative error (ppm)	0.0	4.8	6.2
	Chemical formula	C ₁₈ H ₂₉ N ₂ NaO ₆ P ⁺	C ₁₅ H ₂₄ NNaO ₅ P ⁺	C ₁₂ H ₁₄ N ₂ NaO ₂ ⁺

(IIa), then with the strong electron affinity of the phosphoryl group, the intramolecular oxygen migrates through a five-membered ring phosphorus intermediate to form IIc, which in turn breaks down to form ion II by the extrusion of a fragment HPO₃. In fact, the five-membered phosphorus reaction intermediates of phosphoryl amino acids and peptides have been trapped and determined by ESI-MS/MS in our previous work [49, 50].

It is noteworthy that the above rearrangement only happened with the metallic adducts, but not for the corresponding protonated DIPP-dipeptides (Table 1). This result strongly suggested that the activation of metal ion was

essential for the migration and the rearrangement needs the larger size of Li⁺ or Na⁺ to coordinate both P=O and C=O oxygen atoms to catalyze the oxygen migration via the unusual and some energetically less favorable cleavage pathways. For example, the alkali metal ion adducts of DIPP-Gly-Phe (1) and DIPP-Phe-Ala (9) showed the presence of the ions I and II. This demonstrates that the metal ion having multidentate binding ability can preferentially coordinate with the carbonyl and phosphoryl oxygens and this might be the energetically preferred reaction intermediate to make the carbon atom and phosphorus atom more susceptible to nucleophilic attack. These results are consistent with literature reports [32, 51, 52]. Furthermore, it is worth noting that the relatively more intense rearrangement ion II is observed for Li⁺ and Na⁺ adducts of DIPP-dipeptides, which might be due to the metal ion binding affinity of DIPP-dipeptides following the order Li⁺ > Na⁺ > K⁺ [53, 54]. Since the lithium cation has the highest charge density among all alkali cations because of its smallest size, the radius of the cation increases on going down the alkali metal group, the charge density decreases and the bond distance increases. It seems that both parameters decrease the stabilizing electrostatic interaction between the DIPP-dipeptides and metal ion, and subsequently reduce the formation of the metallic intermediates Ia and IIc (Schemes 6 and 7).

When the ESI-MS/MS data for different DIPP-dipeptides are compared, it is interesting to note that the side chain structures of the C-terminal amino acid residues had considerable effects on the relative abundance of the Li⁺ and Na⁺ adducts ion II. For example, in Compounds 14–17 with C-terminal amino acids containing a hydroxyl group, formation of the Li⁺ and Na⁺ adducts ion II is much more favorable (Table 1). Similarly, the relative intensity of the Li⁺ and Na⁺ adducts ion II is the most abundant (100%) when the C-terminal amino acids are aromatic amino acids, such as Compounds 1, 8, 12, and 13. It seems that Li⁺ and Na⁺ presumably coordinate with the hydroxyl or aryl group of the C-terminal amino acid residues to form an energetically favorable chelate ring by the donation of aromatic



Scheme 3. Possible fragmentation pathways of the deuterium labeled [d_3 -DIPP-Gly-Phe+Na-42]⁺ ion at *m/z* 370.1243

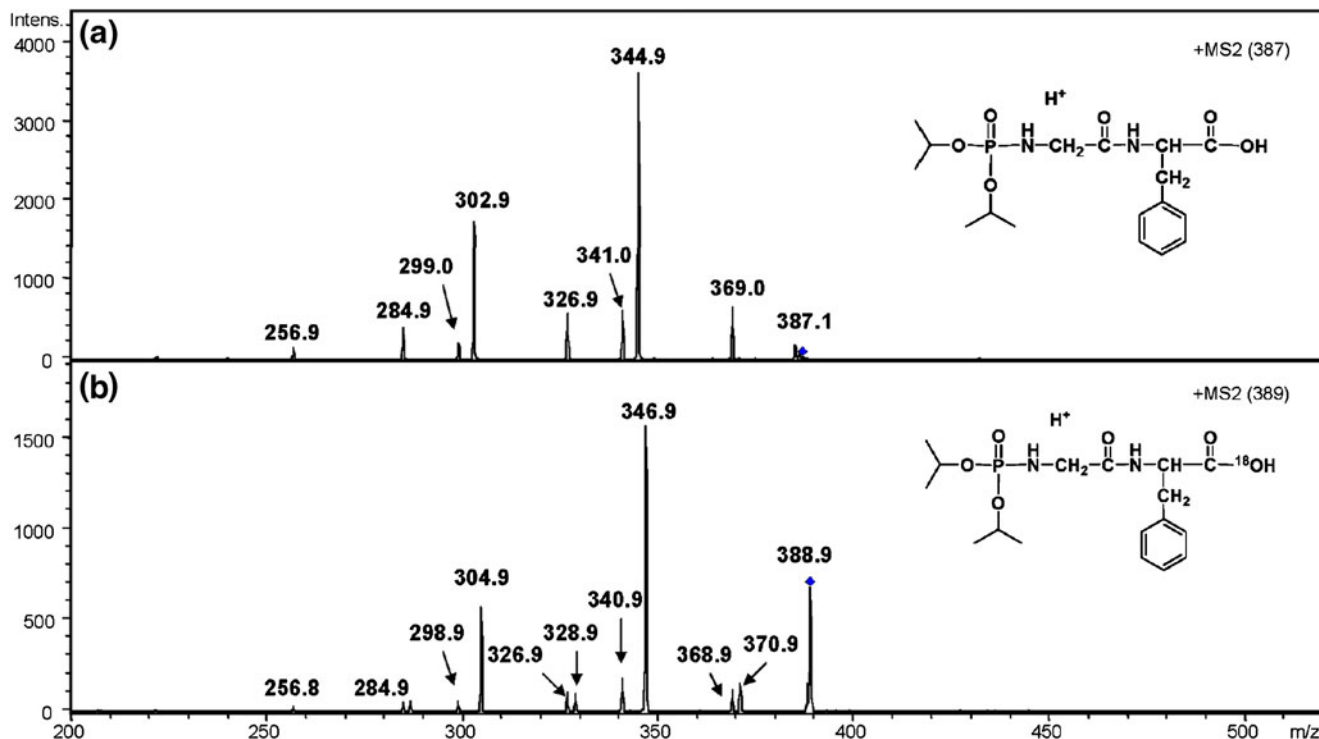
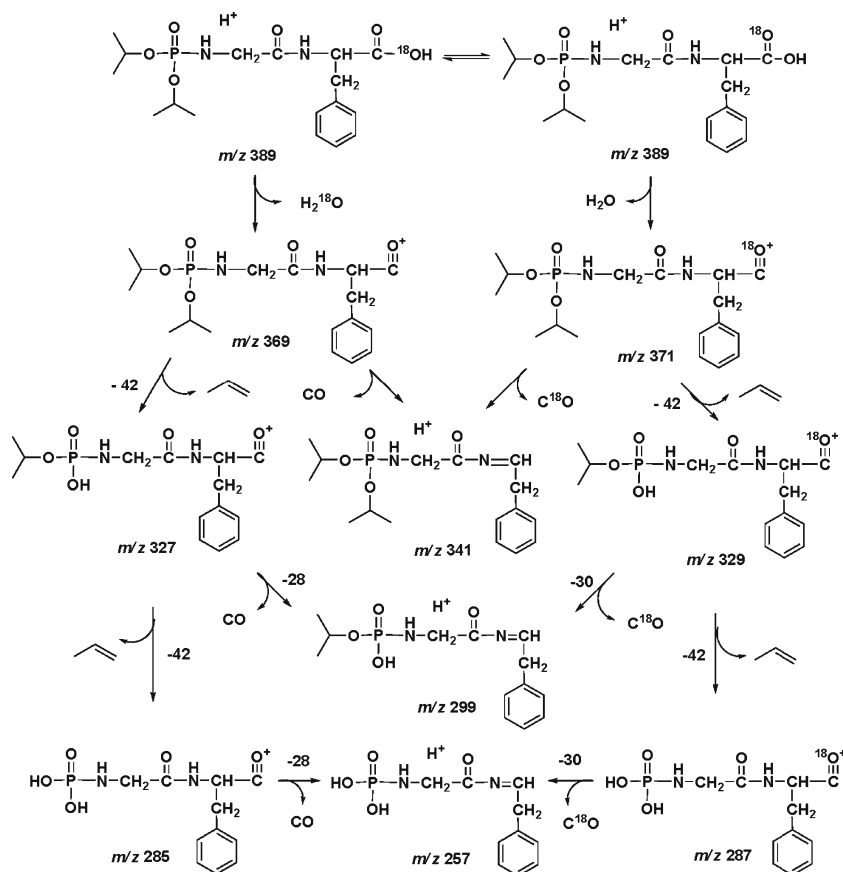
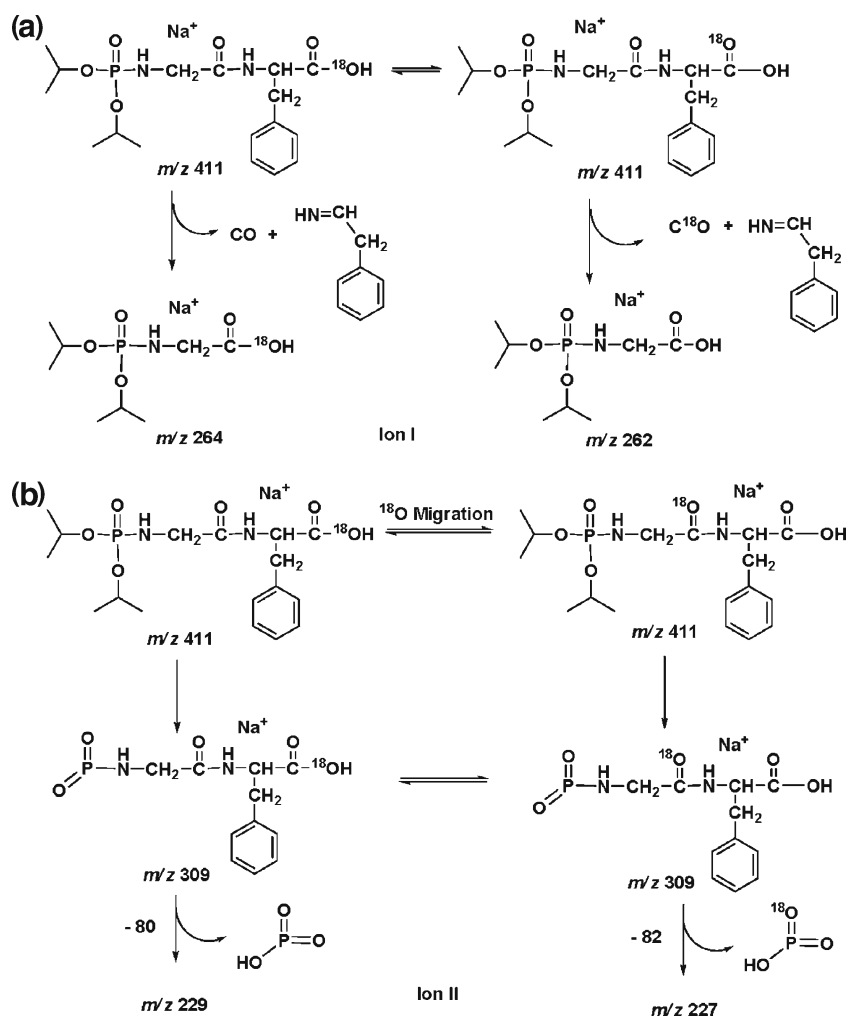


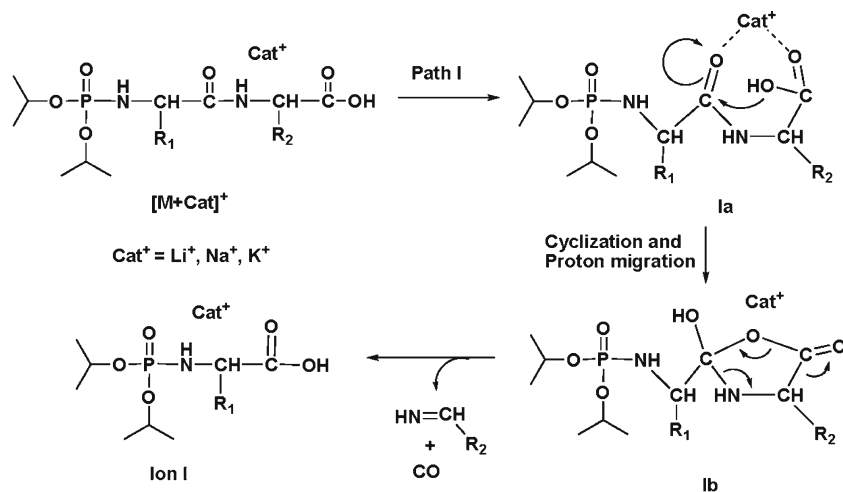
Figure 3. Positive ion ESI-MS/MS spectra of the $[M+H]^+$ ions of the native and isotope labeled DIPP-Gly-Phe. (a) DIPP-Gly-Phe at m/z 387 (Entry 1); (b) DIPP-Gly-Phe- ^{18}OH at m/z 389 (Entry 4)



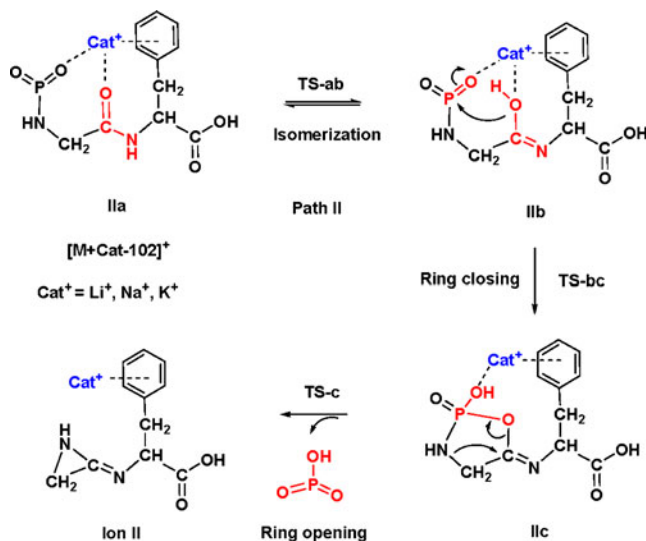
Scheme 4. Possible fragmentation pathways of the protonated DIPP-Gly-Phe- ^{18}OH (Entry 4)



Scheme 5. Fragmentation pathways of the sodium adducts of ^{18}O -labeled DIPP-Gly-Phe- ^{18}OH (Entry 4). **(a)** Formation of the daughter ions at m/z 262 and 264 (Equilibrium between the $\text{C}=\text{}^{18}\text{O}$ and ^{18}OH); **(b)** Formation of the daughter ions at m/z 227 and 229 (The oxygen migration of $\text{C}=\text{}^{18}\text{O}$)



Scheme 6. Proposed rearrangement mechanism for the formation of ion I



Scheme 7. Proposed rearrangement mechanism for the formation of ion II (DIPP-Gly-Phe, Entry 1 as a representative)

π -electrons or lone pair of hydroxyl oxygen atom to the cationic center respectively [55–58], while in our case, K^+ shows such ability to a moderate extent (Scheme 7).

To gain an insight into this oxygen migration steps, we carried out DFT calculations at the B3LYP/6-31 G(d) level by Gaussian 03 program. All species occurring along the rearrangement for the formation of the ion II are depicted in Figure 4. Some of the species involved are also displayed schematically in Scheme 7. The energies (ΔG and ΔE ,

$\text{kcal}\cdot\text{mol}^{-1}$) of the species involved are given along with the energy profile during the multistep reaction from IIa to Ion II $\cdots \text{HPO}_3$ (Figure 4). The calculations indicate that the ring closing step from IIb to IIc, namely concerted proton transfer and cyclization is the rate-determining reaction step. In addition, this ring closing step is also a thermodynamically favorable process in which the relative free energies of this process are: $-2.9 \text{ kcal}\cdot\text{mol}^{-1}$ for Li^+ , $1.0 \text{ kcal}\cdot\text{mol}^{-1}$ for Na^+ , and $9.4 \text{ kcal}\cdot\text{mol}^{-1}$ for K^+ . Furthermore, the transition state

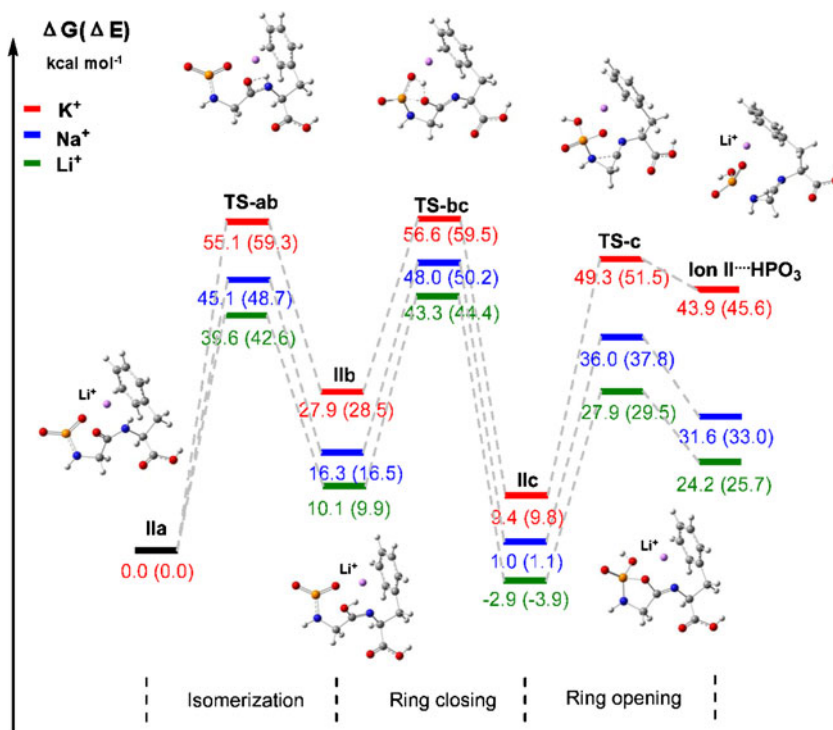


Figure 4. Free energies (ΔG), relative energies (ΔE , in parentheses) and the optimized structures (Li^+ adducts) for the formation of ion II corresponded to Scheme 7 (Entry 1, $\text{Cat}^+ = \text{Li}^+, \text{Na}^+, \text{and } \text{K}^+$). The energies of all different species were relative to that of IIa for each metal ion complex. The energies are given in $\text{kcal}\cdot\text{mol}^{-1}$

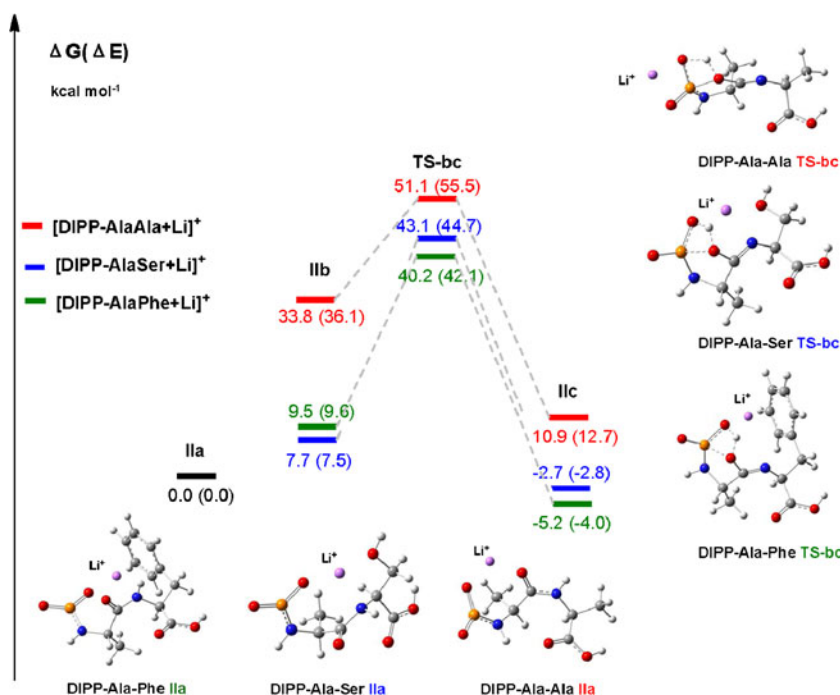


Figure 5. Comparison of free energies (ΔG , kcal·mol⁻¹) and relative energies (ΔE , kcal·mol⁻¹, in parentheses) for the formation of intermediate IIc between Entry 5, 8, and 14. The bottom and right were the optimized structures for the lithiated IIa and TS-bc, respectively. The energies were relative to that of IIa for each metal ion complex

TS-bc corresponding to this process is located and depicted in Figure 4. As can be seen, the transferring proton is somewhere in between the two oxygen atoms, and the distance between the carbonyl oxygen and phosphorus atom (1.858 Å) for TS-bc is less than that of IIb (3.167 Å) but longer than IIc (1.662 Å) (Figure S1), indicating that proton transfer and nucleophilic attack might happen simultaneously as a result of a relatively strong charge transfer interaction involving the lone pair of oxygen atom and the partially positively charged phosphorus atom. The order of the overall barrier is: K⁺ (56.6 kcal·mol⁻¹) > Na⁺ (48.0 kcal·mol⁻¹) > Li⁺ (43.3 kcal·mol⁻¹), in line with the experimental observations that Li⁺ can catalyze the oxygen migration more efficiently than K⁺. It should be also pointed here that the relative high free energy of the Ion II (Ring opening) might be due to the large strain of the three-membered ring structure, which could further undergo ring-open process and lead to thermodynamically favorable product containing a N=C–N=C or N=C–C=N unit depending on which bond (C–C or C–N bond) is cleaved.

In order to further clarify the effect of the amino acid side chains, we selectively optimized the rate-determining step in the reaction mechanism for the lithiated DIPP-dipeptides 5, 8, and 14 with different C-terminal amino acid residues. As shown in Figure 5, the order of the calculated barriers for the formation of the intermediate IIc are: DIPP-Ala-Ala (Entry 5, 51.1 kcal·mol⁻¹) > DIPP-Ala-Ser (Entry 14, 43.1 kcal·mol⁻¹) > DIPP-Ala-Phe (Entry 8, 40.2 kcal·mol⁻¹), in line with the observed relative abundance of rearrangement ions II in

ion-trap tandem mass spectrometer (Table 1). Furthermore, the structures of the lithiated intermediates IIa and transition state TS-bc depicted in Figure 5 demonstrated that the lithium cation could spatially bind to the phenyl group (DIPP-Gly-Phe and DIPP-Ala-Phe) or hydroxyl group (DIPP-Ala-Ser) of the C-terminal amino acid residues respectively. However, such a stabilization can not be achieved in DIPP-Ala-Ala with a methyl side chain. All in all, the calculations suggest that the formation of ions II depends on the nature of the metal cations and specific structures of the amino acid residues.

Further evidence for the generation of ion II is shown by comparing the ESI-MS/MS data of several pairs of formula isomers, such as DIPP-Ala-Phe (8)/DIPP-Phe-Ala (9), DIPP-Gly-Phe (1)/DIPP-Phe-Gly (10), and DIPP-Phe-Val (11)/DIPP-Val-Phe (12) having a phenylalanine residue at the C- or N-terminal respectively (Table 1). For example, for compounds 8 and 9, it is notable that both of them yield the same formula (C₁₂H₁₄N₂NaO₂, Table 2) for ion II at *m/z* 241, but with 100% and 55% abundance respectively. It means that the C-terminal aromatic amino acid has a stronger π -system stabilization effect for ion II than that of the N-terminal one. On the other hand, for the generation of ion I, there is not much difference between the corresponding Li⁺ and Na⁺ adducts. These data are consistent with the rearrangement mechanism proposed in Schemes 6 and 7. Consequently, these results show that ESI-MS/MS is a useful tool for isomeric differentiation through collisionally induced dissociation of the metal ion complexes [59, 60].

Conclusions

In summary, the collision-induced dissociation reactions of a variety of *N*-phosphoryl dipeptides have been studied in detail using MS/MS experiments, isotope (^{18}O , ^{15}N , and ^2H) labeling, accurate mass measurements and DFT calculations. The alkali metal cations, especially for Li^+ and Na^+ , can catalyze a carbonyl oxygen migration through a phosphoryl group participating five-membered ring intermediate. None of the oxygen migrations is observed for the corresponding protonated *N*-phosphoryl dipeptides. This study indicates that the Group I metal ions can play an essential role for the rearrangement of a phosphorylated peptide or protein. Furthermore, when different *N*-phosphoryl dipeptides are compared, it is found that the C-terminal amino acid with potential coordinating side chains, such as the hydroxyl group or aromatic ring, the formation of rearrangement ion for carbonyl oxygen migration is more favorable. These results show that ESI-MS is a useful tool for structural determination of phosphorylated dipeptides. In addition, the discovery of potential metal cation (Li^+ or Na^+) coordination between the phosphoryl group and the amino acid residue side chains may provide new insights into the mechanism for molecular recognition through the interaction between the P=O group and protein side chains by the action of metal ions.

Acknowledgments

The authors acknowledge financial supports from the Major Program of National Natural Science Foundation of China (no. 20732004), the National Natural Science Foundation of China (no. 20972130 and no. 21075103), and startup funding for J.Z. by Xiamen University. They thank Professor G. M. Blackburn for helpful discussions and suggestions.

References

- Zhao, Y.F., Cao, P.S.: Phosphoryl amino acids: common origin for nucleic acids and protein. *J. Biol. Phys.* **20**, 283–287 (1994)
- Fu, H., Li, Z.Z., Zhao, Y.F., Tu, G.Z.: Oligomerization of N, O-Bis (Trimethylsilyl)- α -amino acids into peptides mediated by *o*-phenylene phosphorochloridate. *J. Am. Chem. Soc.* **121**, 291–295 (1999)
- Pascal, R., Boiteau, L., Commeyras, A.: From the prebiotic synthesis of α -amino acids towards a primitive translation apparatus for the synthesis of peptides. *Top. Curr. Chem.* **259**, 69–122 (2005)
- Cheng, C.M., Liu, X.H., Li, Y.M., Ma, Y., Tan, B., Wan, R., Zhao, Y.F.: *N*-phosphoryl amino acids and biomolecular origins. *Orig. Life Evol. Biosph.* **34**, 455–464 (2004)
- Landweber, L.F.: Testing ancient RNA-protein interactions. *Proc. Natl. Acad. Sci. U.S.A.* **96**, 11067–11068 (1999)
- Zhou, W.H., Ju, Y., Zhao, Y.F., Wang, Q.G., Luo, G.A.: Simultaneous formation of peptides and nucleotides from *N*-phosphothreonine. *Orig. Life Evol. Biosph.* **26**, 547–560 (1996)
- Li, W., Ma, Y., Zhao, Y.F.: Penta-coordinated phosphorus structure analysis on kinases. *Sci. China Ser. B Chem.* **47**, 420–427 (2004)
- Ni, F., Li, W., Li, Y.M., Zhao, Y.F.: Analysis of the phosphoryl transfer mechanism of c-AMP dependent protein kinase (PKA) by penta-coordinate phosphoric transition state theory. *Curr. Protein Pept. Sci.* **6**, 437–442 (2005)
- Gao, X., Liu, Y., Xu, P.X., Cai, Y.M., Zhao, Y.F.: α -amino acid behaves differently from β - or γ -amino acids as treated by trimetaphosphate. *Amino Acids* **34**, 47–53 (2008)
- Li, Y.M., Zhang, D.Q., Zhang, H.W., Ji, G.J., Zhao, Y.F.: β -carboxyl catalytic effect of *N*-phosphoryl aspartic acid. *Bioorg. Chem.* **20**, 285–295 (1992)
- Chen, Z.Z., Tan, B., Li, Y.M., Zhao, Y.F.: Activity difference between α -COOH and β -COOH in *N*-phosphoryl aspartic acids. *J. Org. Chem.* **68**, 4052–4058 (2003)
- Xue, C.B., Yin, Y.W., Zhao, Y.F.: Studies on phosphoserine and phosphothreonine derivatives. *Tetrahedron Lett.* **29**, 1145–1148 (1988)
- Chen, Z.Z., Li, Y.M., Wang, H.Y., Du, J.T., Zhao, Y.F.: Theoretical study on the rearrangement of β -OH and γ -OH in ESI mass spectrometry by *N*-phosphorylation. *J. Phys. Chem. A* **108**, 7686–7690 (2004)
- Poncz, L., Gerken, T.A., Dearborn, D.G., Grobelny, D., Galardy, R.E.: Inhibition of the elastase of *Pseudomonas aeruginosa* by *N*-phosphoryl dipeptides and kinetics of spontaneous hydrolysis of the inhibitors. *Biochemistry* **23**, 2766–2772 (1984)
- Westheimer, F.H.: Why nature chose phosphates. *Science* **235**, 1173–1178 (1987)
- Hunter, T.: Signaling-2000 and beyond. *Cell* **100**, 113–127 (2000)
- Johnson, L.N., Lewis, R.: Structural basis for control by phosphorylation. *Chem. Rev.* **101**, 2209–2242 (2001)
- Adams, J.A.: Kinetic and catalytic mechanism of protein kinases. *Chem. Rev.* **101**, 227–2290 (2001)
- Yamashita, M., Fenn, J.B.: Negative ion production with the electrospray ion source. *J. Phys. Chem.* **88**, 4671–4675 (1984)
- Schalley, C.A.: Molecular recognition and supramolecular chemistry in the gas phase. *Mass Spectrom. Rev.* **20**, 253–309 (2001)
- Chen, X.L., Qu, L.B., Zhang, T., Liu, H.X., Yu, F., Yu, Y.Z., Liao, X.C., Zhao, Y.F.: The nature of phosphorylated chrysin–protein interactions involved in noncovalent complex formation by electrospray ionization mass spectrometry. *Anal. Chem.* **76**, 211–217 (2004)
- Schlosser, A., Pipkorn, R., Bossemeyer, D., Lehmann, W.D.: Analysis of protein phosphorylation by a combination of elastase digestion and neutral loss tandem mass spectrometry. *Anal. Chem.* **73**, 170–176 (2001)
- Barlow, C.K., O’Hair, R.A.J.: Gas-phase peptide fragmentation: how understanding the fundamentals provides a springboard to developing new chemistry and novel proteomic tools. *J. Mass Spectrom.* **43**, 1301–1319 (2008)
- Chu, I.K., Guo, X., Lau, T.C., Siu, K.W.M.: Sequencing of argenitinated peptides by means of electrospray tandem mass spectrometry. *Anal. Chem.* **71**, 2364–2372 (1999)
- Lin, T., Payne, A.H., Glish, G.L.: Dissociation pathways of alkalicationized peptides: opportunities for C-terminal peptide sequencing. *J. Am. Soc. Mass Spectrom.* **12**, 497–504 (2001)
- Lin, T., Glish, G.L.: C-terminal peptide sequencing via multistage mass spectrometry. *Anal. Chem.* **70**, 5162–5165 (1998)
- Operti, L., Rabezzana, R.: Gas-phase ion thermochemistry in organometallic systems. *Mass Spectrom. Rev.* **22**, 407–428 (2003)
- Bao, J.Y., Ai, H.W., Fu, H., Jiang, Y.Y., Zhao, Y.F., Huang, C.: Peptide sequencing through *N*-terminal phosphorylation and electrospray ionization mass spectrometry. *J. Mass Spectrom.* **40**, 772–776 (2005)
- Wang, F., Fu, H., Jiang, Y.Y., Zhao, Y.F.: A picomole-scale method for rapid peptide sequencing through convenient and efficient *N*-terminal phosphorylation and electrospray ionization mass spectrometry. *J. Am. Soc. Mass Spectrom.* **17**, 995–999 (2006)
- Chen, J., Chen, Y., Jiang, Y., Fu, H., Zhao, Y.F.: Rearrangement of P–N and P–O bonds in mass spectra of *N*-diisopropoxyphosphoryl amino acids/alcohols. *Rapid Commun. Spectrom.* **15**, 1936–1940 (2001)
- Chen, J., Chen, Y., Niu, Y.Y., Fu, H., Zhao, Y.F.: A carbonyl oxygen migration in electrospray ionization mass spectrometry and its application in differentiating α - and β -alanyl peptides. *J. Mass Spectrom.* **37**, 934–939 (2002)
- Chen, Y., Yin, Y.W., Sun, X.B., Liu, X.H., Wang, H.Y., Zhao, Y.F.: A novel rearrangement in electrospray ionization mass spectrometry of amino acids ester cyclohexyl phosphoramidates of AZT. *J. Mass Spectrom.* **40**, 636–641 (2005)
- Ji, G.J., Xue, C.B., Zeng, J.N., Li, L.P., Chai, W.G., Zhao, Y.F.: Synthesis of *N*-(Diisopropoxyphosphoryl) amino acids and peptides. *Synthesis* **6**, 444–448 (1988)
- Tang, G., Zhou, G.J., Ni, F., Hu, L.M., Zhao, Y.F.: ^{31}P NMR and ESI-MS studies on some intermediates of the peptide coupling reagents triphenyl-chlorophosphoranes. *Chin. Chem. Lett.* **16**, 385–388 (2005)

35. Ulibarri, G., Choret, N., Bigg, D.C.H.: Activation of imidazolides using methyl trifluoromethanesulfonate: a convenient method for the preparation of hindered esters and amides. *Synthesis* **11**, 1286–1288 (1996)
36. Becke, A.D.: Density-functional thermochemistry. III. The role of exact exchange. *J. Chem. Phys.* **98**, 5648–5652 (1993)
37. Miehlich, B., Savin, A., Stoll, H., Preuss, H.: Results obtained with the correlation energy density functionals of Becke and Lee, Yang, and Parr. *Chem. Phys. Lett.* **157**, 200–206 (1989)
38. Lee, C., Yang, W., Parr, G.: Development of the colle-salvetti correlation-energy formula into a functional of the electron density. *Phys. Rev. B* **37**, 785–789 (1988)
39. Fukui, K.: Formulation of the reaction coordinate. *J. Phys. Chem.* **74**, 4161–4163 (1970)
40. Fukui, K.: The path of chemical reactions-the IRC approach. *Acc. Chem. Res.* **14**, 363–368 (1981)
41. Frisch, M.J., Trucks, G.W., Schlegel, H.B., Scuseria, G.E., Robb, M.A., Cheeseman, J.R., Montgomery Jr., J.A., Vreven, T., Kudin, K.N., Burant, J.C., Millam, J.M., Iyengar, S.S., Tomasi, J., Barone, V., Mennucci, B., Cossi, M., Scalmani, G., Rega, N., Petersson, G.A., Nakatsuji, H., Hada, M., Ehara, M., Toyota, K., Fukuda, R., Hasegawa, J., Ishida, M., Nakajima, T., Honda, Y., Kitao, O., Nakai, H., Klene, M., Li, X., Knox, J.E., Hratchian, H.P., Cross, J.B., Bakken, V., Adamo, C., Jaramillo, J., Gomperts, R., Stratmann, R.E., Yazyev, O., Austin, A.J., Cammi, R., Pomelli, C., Ochterski, J.W., Ayala, P.Y., Morokuma, K., Voth, G.A., Salvador, P., Dannenberg, J.J., Zakrzewski, V.G., Dapprich, S., Daniels, A.D., Strain, M.C., Farkas, O., Malick, D.K., Rabuck, A.D., Raghavachari, K., Foresman, J.B., Ortiz, J.V., Cui, Q., Baboul, A.G., Clifford, S., Cioslowski, J., Stefanov, B.B., Liu, G., Liashenko, A., Piskorz, P., Komaromi, I., Martin, R.L., Fox, D.J., Keith, T., Al-Laham, M.A., Peng, C.Y., Nanayakkara, A., Challacombe, M., Gill, P.M.W., Johnson, B., Chen, W., Wong, M.W., Gonzalez, C., Pople, J.A.: Gaussian 03, revision E.01. Gaussian, Inc, Wallingford (2004)
42. Ballard, K.D., Gaskell, S.J.: Intramolecular [¹⁸O] isotopic exchange in the gas phase observed during the tandem mass spectrometric analysis of peptides. *J. Am. Chem. Soc.* **114**, 64–71 (1992)
43. Teesch, L.M., Adams, J.: Fragmentations of gas-phase complexes between alkali metal ions and peptides: metal ion binding to carbonyl oxygens and other neutral functional groups. *J. Am. Chem. Soc.* **113**, 812–820 (1991)
44. Grese, R.P., Cerny, R.L., Gross, M.L.: Metal ion–peptide interactions in the gas phase: a tandem mass spectrometry study of alkali metal cationized peptides. *J. Am. Chem. Soc.* **111**, 2835–2842 (1989)
45. Feng, W.Y., Gronert, S., Fletcher, K.A., Warres, A., Lebrilla, C.B.: The mechanism of C-terminal fragmentations in alkali metal ion complexes of peptides. *Int. J. Mass Spectrom.* **222**, 117–134 (2003)
46. Bythell, B.J., Suhai, S., Somogyi, A., Paizs, B.: Proton-driven amide bond-cleavage pathways of gas-phase peptide ions lacking mobile protons. *J. Am. Chem. Soc.* **131**, 14057–14065 (2009)
47. Farrugia, J.M., O'Hair, R.A.J.: Involvement of salt bridges in a novel gas phase rearrangement of protonated arginine-containing dipeptides which precedes fragmentation. *Int. J. Mass Spectrom.* **222**, 229–242 (2003)
48. Forbes, M.W., Jockusch, R.A., Young, A.B., Harrison, A.G.: Fragmentation of protonated dipeptides containing arginine. Effect of activation method. *J. Am. Soc. Mass Spectrom.* **18**, 1959–1966 (2007)
49. Qiang, L.M., Liu, R.Y., Xie, Y.L., Cao, S.X., Liao, X.C., Zhao, Y.F.: A carbonyl oxygen migration of *N*-phosphoryl dipeptide methyl esters containing β -alanine or γ -amino butyric acids in electrospray ionization mass spectrometry. *Int. J. Mass Spectrom.* **272**, 204–207 (2008)
50. Gao, X., Ni, F., Bao, J., Liu, Y., Xu, P.X., Zhao, Y.F.: Formation of cyclic acylphosphoramidates in mass spectra of *N*-monoalkoxyphosphoryl amino acids using electrospray ionization tandem mass spectrometry. *J. Mass Spectrom.* **45**, 779–787 (2010)
51. Tang, X.J., Ens, W., Standing, K.G., Westmore, J.B.: Daughter ion mass spectra from cationized molecules of small oligopeptides in a reflecting time-of-flight mass spectrometer. *Anal. Chem.* **60**, 1791–1799 (1988)
52. Chen, Y., Zhang, J.C., Chen, J., Cao, X.Y., Wang, J., Zhao, Y.F.: Sensitivity improvement of amino acids by *N*-terminal diisopropylxophosphorylation in electrospray ionization mass spectrometry. *Rapid Commun. Spectrom.* **18**, 469–473 (2004)
53. Abirami, S., Wong, C.C.L., Tsang, C.W., Ma, N.L.: Dissociation of alkaliated alanine in the gas phase: the role of the metal cation. *Chem. Eur. J.* **11**, 5289–5301 (2005)
54. Sudha, R., Panda, M., Chandrasekhar, J., Balaram, P.: Structural effects on the formation of proton and alkali metal ion adducts of apolar, neutral peptides: electrospray ionization mass spectrometry and Ab Initio theoretical studies. *Chem. Eur. J.* **8**, 4980–4991 (2002)
55. Hoyau, S., Norman, K., McMahon, T.B., Ohanessian, G.: A quantitative basis for a scale of na affinities of organic and small molecules in the gas phase. *J. Am. Chem. Soc.* **121**, 8864–8875 (1999)
56. Ryzhov, V., Dunbar, R.C., Cerda, B.A., Wesdemiotis, C.: Cation- π effects in the complexation of Na⁺ and K⁺ with Phe, Try, and Trp in the gase phase. *J. Am. Soc. Mass Spectrom.* **11**, 1037–1046 (2000)
57. Wang, P., Wesdemiotis, C., Kapota, C., Ohanessian, G.: The sodium ion affinities of simple Di-, Tri-, and tetrapeptides. *J. Am. Soc. Mass Spectrom.* **18**, 541–552 (2007)
58. Feng, W.Y., Gronert, S., Lebrilla, C.B.: Lithium and sodium ion binding energies of *N*-acetyl and *N*-glycyl amino acids. *J. Am. Chem. Soc.* **121**, 1365–1371 (1999)
59. Pingitore, F., Wesdemiotis, C.: Characterization of dipeptide isomers by tandem mass spectrometry of their mono- versus dilithiated complexes. *Anal. Chem.* **77**, 1796–1806 (2005)
60. Zhang, J.M., Brodbelt, J.S.: Silver complexation and tandem mass spectrometry for differentiation of isomeric flavonoid diglycosides. *Anal. Chem.* **77**, 1761–1770 (2005)